

Arrival Management for High-density Vertiport and Terminal Airspace Operations

Shulu Chen, ATCA student member
Peng Wei
George Washington University
Washington, D.C. 20052

Paul Krois
Joseph Block
Paul Cobb
Gano Chatterji
Cherie Kurian
Crown Consulting, Inc.
Arlington, VA 22202

Abstract

Vertiports will play a vital role in transporting passengers and cargo in an urban air environment. In this confined airspace, as traffic volume increases, the arrival demand may exceed the vertiport's capacity, resulting in vertiport terminal area conflicts and efficiency concerns. To address this challenge, we propose a terminal airspace management automation tool that integrates seamlessly with a vertiport's surface operations. The terminal airspace structure may introduce bottleneck points, such as the touchdown and lift-off areas, common standard arrival routes, and metering fixes. To optimize traffic flow at these bottleneck points and deconflict arrival aircraft in the terminal airspace, we developed an optimization-based scheduling algorithm for strategic conflict management, as well as a maneuver advisory algorithm to provide speed and holding advisories to meet the required time of arrival from the scheduling algorithm. Our results suggest that implementing holding patterns in the structured terminal airspace using these algorithms can mitigate conflicts in high-density vertiport and terminal airspace operations. Additionally, our study provides early insights into the interactions between the arrival management automation and human operators.

1. Introduction

Urban traffic demands have been forecast to steadily increasing for decades, and there seems to be no end in sight to this growth. In response, further development of urban airspace is necessary to expand traffic capacity and offer more travel options. One key direction of this development is advanced air mobility (AAM), including use of electric take-off and landing (eVTOL) aircraft for cargo transportation and passenger air taxis. To support AAM, big cities will need to allocate an adequate number of vertiports and design a new airspace structure with an air traffic management (ATM) system that is compatible with AAM. The AAM system features higher traffic throughput rates, smaller terminal airspace, and mitigation of uncertainty in operations. In this paper, we describe the design of new airspace, ATM procedures and automation tools to overcome these challenges.

The Federal Aviation Administration (FAA) poses a future information-centric vision of the National Airspace System (NAS) that includes vertiports as part of the physical infrastructure (The Federal Aviation Administration, Charting Aviation's Future: Operations in an Info-Centric National Airspace System 2022). The FAA provides interim guidance on advanced vertiport design and operation that will include autonomy and high-tempo operational facilities (The Federal Aviation Administration, Engineering Brief No. 105, Vertiport Design 2022). Vertiports will serve a critical role for moving passengers and cargo in an urban environment with increasingly dense traffic volumes and airspace complexity.

Traffic volume and complexity of terminal airspace leads to bottlenecks that limit traffic flow throughput and introduces delays that impact flight schedules. This is analogous to today's high density terminal operations employing sequencing and spacing for metering arrival traffic to airports. In contrast, vertiports as part of urban air mobility (UAM), which is a sub-market of AAM, potentially involve more dense traffic flows in increasingly complex airspace with vehicles in closer proximity.

Research by the National Aeronautics and Space Administration (NASA) showed a range of airspace considerations associated with airspace including airspace class, traffic volume, no fly zones, multiple approach and departure routes available, and metropolitan airspace strategy (Mendonca 2022). These were some of the more than 450 considerations identified applicable to siting, designing, and operating a vertiport. In addition, an analysis of demand capacity balancing at vertiports found more effective strategic conflict management by using assigned flight speeds for different route segments and using estimated time of arrival at significant waypoints to reduce use of tactical separation (Lee 2022).

A Vertiport Human Automation Teaming Toolbox (V-HATT) was prototyped to simulate vertiport airside operations with direct human vertiport operator oversight (Crown Consulting 2023). This paper describes the automation tools to enable teaming with the human vertiport operator to optimize throughput management as a core component of future vertiport operational systems. A vertiport depicting traffic flows, touchdown and liftoff (TLOF) pads, final approach and takeoff (FATO) areas, and passenger and cargo walkways is shown in Figure 1.

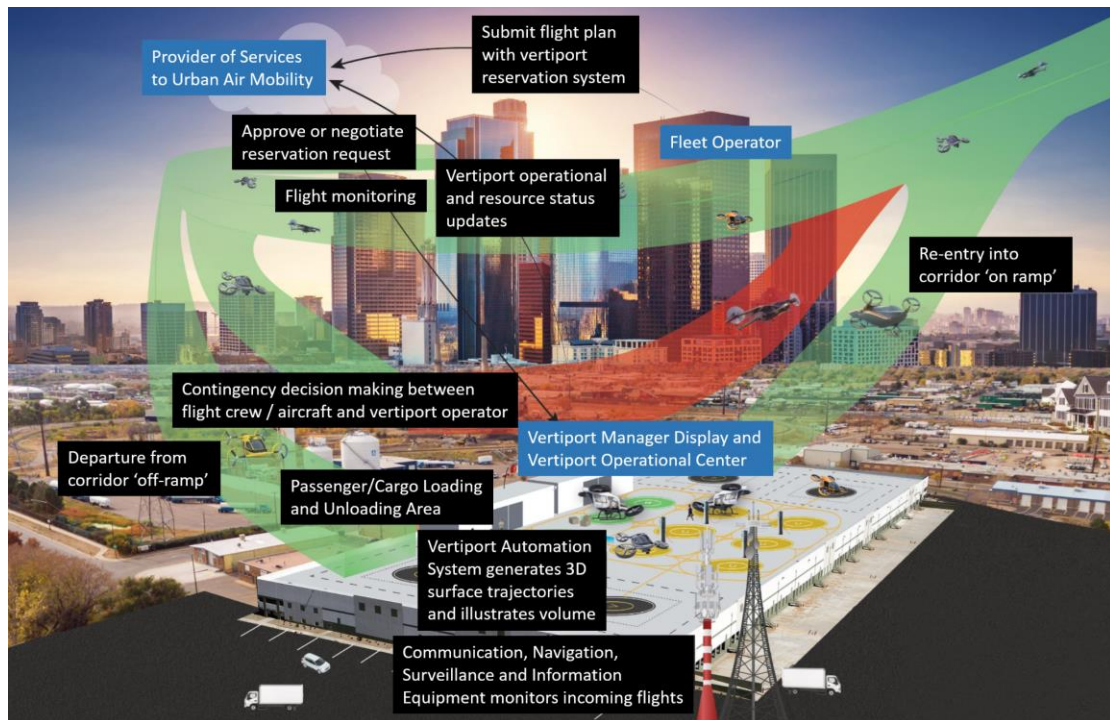


Figure 1: Vertiport and airside operations (*Northeast UAS Airspace Integration Research Alliance 2021*)

2. Design of Vertiport Terminal Airspace

For purposes of this paper, the conceptual design of terminal airspace is shown in Figure 2. The focus of this paper is on the safe separation for the arrival traffic flow. The green lines represent the routes of four incoming aircraft. In this vertiport terminal airspace setting, the aircraft enters the terminal airspace by first reaching the entry fix, then merging into the metering gate before finally landing at the vertiport. Four functional circles have been designed around the vertiport to support this arrival process.

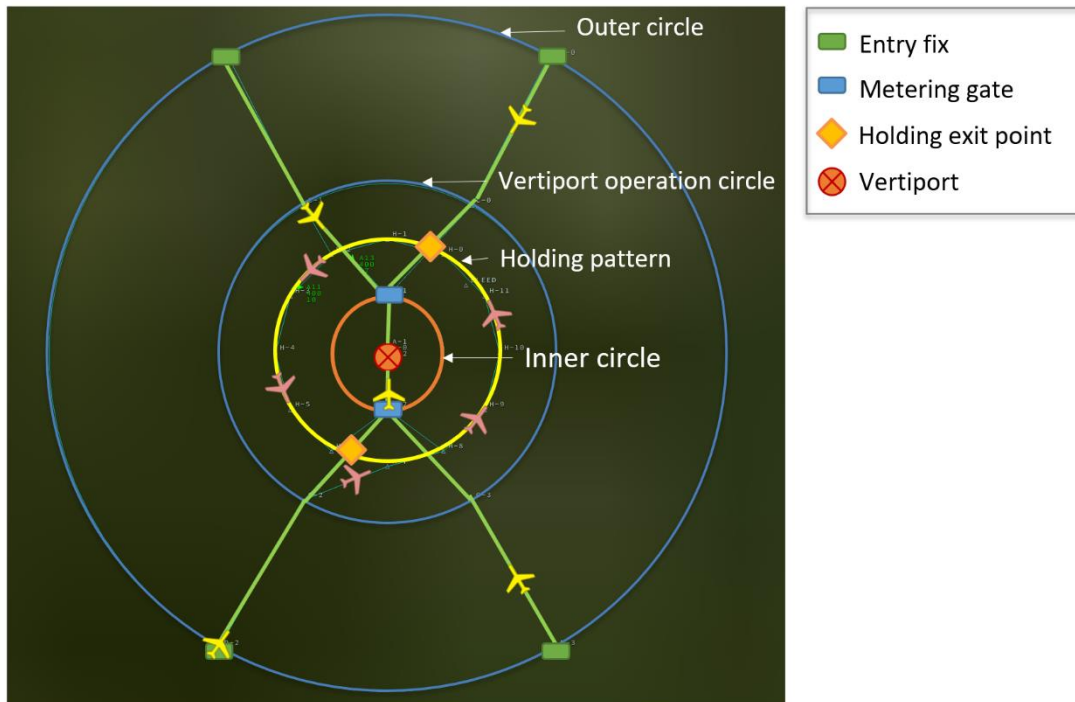


Figure 2: Vertiport terminal airspace design

- Outer circle.** Based on the assumption, the outer circle is defined as where the vertiport operator first detects arrival aircraft. The size of the outer circle depends on the terminal radar capability. Four entering fixes are located around this circle as the initial vertiport detection points. We assume that it is not necessary for vertiport operator to manage aircraft outside this circle.
- Vertiport operation circle.** With a radius of 1.5 nautical miles, the vertiport operation circle is where aircraft execute given operations. The decision buffer zone is the area between the outer circle and the vertiport operation circle. When aircraft are within this zone, automated systems and human operators may issue commands such as speeding up, slowing down, entering a holding pattern, or proceeding on course based on the current traffic density and vertiport status. Once an aircraft passes through the vertiport operation circle, it will execute the required maneuvers. Note that imposing a holding time for an eVTOL aircraft refers to a change in trajectory using some minimal speed to absorb a time delay and not to a hover that involves a higher level of battery power.
- Holding pattern.** A holding pattern is a circular area with a radius of 1 nautical mile that is used as a waiting area to absorb in-air delays issued by the automation or vertiport operator. When arrival demand is higher than the vertiport capacity, some aircraft may be asked to fly within the holding pattern. In this paper, we assume all aircraft are flying point to point, thus, to simplify the control process, the holding pattern is divided into several flying segments by corresponding waypoints, and automation will assign the number of segments that an aircraft must fly based on its calculated waiting time and speed. Once the arrival TLOF becomes available or traffic is relieved, the aircraft will continue flying around the holding

pattern until it reaches the closest holding exit point, at which point it will proceed to the metering gate and prepare for the landing procedure.

- **Inner circle.** The radius of the inner circle is 0.5 nautical mile. When an aircraft enters this area through the metering gate, it will follow a predetermined landing approach with a fixed schedule.

3. Technical Approach

3.1 Automated System Workflow

As the automation part of V-HATT, we constructed a simulation environment for verifying the feasibility and reliability of the system. In this paper, we use BlueSky (Hoekstra 2016) as the simulation core to model the aircraft operations.

At the start of the simulation, we assumed that all aircraft must submit a landing request to the vertiport. The request includes the estimated time of arrival (ETA) and the route ID. The vertiport operator automatically accepts aircraft and does not have the authority to hold aircraft outside the terminal airspace. In other words, the time of appearance of aircraft is fixed. Arrival of unscheduled aircraft was not included in this analysis.

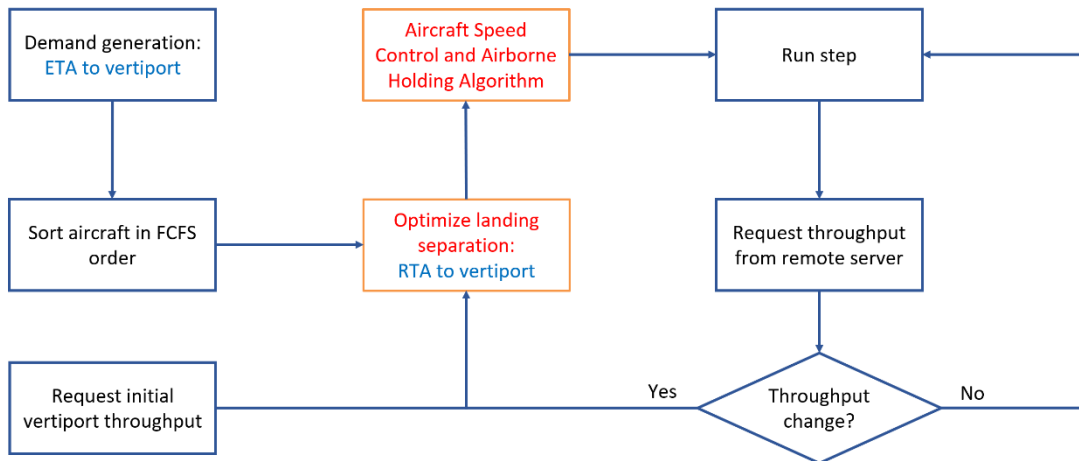


Figure 3: Airborne automation workflow

Figure 3 illustrates the workflow of the automation system. When the automation system receives the estimated time of arrival (ETA), it will create an arrival queue on first come first serve order. Next, an optimization method is used to calculate the required time of arrival (RTA) for each aircraft based on the given ETA, the initial vertiport throughput, and the aircraft's remaining battery life. Based on the time gap between the ETA and the RTA, the automation system applies a speed control and airborne holding algorithm to determine the desired speed and waiting time, if applicable, for each aircraft. When the simulation begins, an aircraft will either adjust to the desired speed or detour to a holding pattern after passing through the vertiport operation circle. The automation system will continuously monitor the vertiport status and recalculate the RTAs and aircraft maneuvers if the vertiport throughput changes.

3.2 Scheduling Algorithm

In this paper, we extended the methods (Pradeep and Wei 2018) to develop an optimization-based scheduling algorithm for the integrated vertiport and terminal airspace structure. Specifically, the aircraft scheduling problem is formulated as a mixed-integer linear program (MILP):

$$\min \sum_{i \in \mathcal{I}} T_i^{RTA} \quad (1)$$

$$\text{s.t. } T_i^{RTA} - T_j^{RTA} \geq \Delta T \quad \forall i > j \quad (2)$$

$$T_i^{RTA} \geq T_i^{EST} \quad \forall i \in \mathcal{I} \quad (3)$$

$$T_i^{EST} = T_i^{ETA} + t_i^c \frac{v_i^c}{v_i^{max}} - t_i^c \quad \forall i \in \mathcal{I} \quad (4)$$

$$T_i^{RTA} \leq T_i^{LST} \quad \forall i \in \mathcal{I} \quad (5)$$

$$T_i^{LST} = T_i^{ETA} + U_i \quad \forall i \in \mathcal{I} \quad (6)$$

The objective of this problem is to minimize the total required time of arrival (RTA), with three constraints. Constraint (2) represents that the optimized landing point T^{RTA} of any two aircraft should be larger than a time buffer ΔT . This time buffer is determined by the current vertiport throughput. Constraints (3) and (4) provide a lower bound of the RTA, noted as the earliest time of arrival T^{EST} , which is calculated based on the flight performance parameters, cruise speed v^c and maximum speed v^{max} , as well as the flying time on cruise speed t^c to the metering gate. Constraints (5) and (6) provide an upper bound of the RTA, noted as the latest time of arrival T^{LST} , which is based on the consideration of the remaining battery energy U .

The problem is solved with a commonly used commercial optimization solver called Gurobi, which is available via the Python library.

3.3 Aircraft Speed Control and Airborne Holding Algorithm

Given the ETA and RTA, the next challenge is to control the aircraft to reach the required time of arrival. To address this problem, we developed an aircraft speed control and airborne holding algorithm that determines the desired speed and holding time for arriving aircraft. This algorithm allows for precise control over the aircraft's speed and position, ensuring that it arrives at its destination on time.

Algorithm 1: Aircraft Speed Control and Airborne Holding Algorithm

```
1 foreach aircraft  $i$  do
2   Calculate time gap:  $t_i^g = T_i^{RTA} - T_i^{ETA}$ 
3   Calculate actual flying time:  $t_i^a = t_i^g + t_i^c$ 
4   Calculate desired speed:  $v_i^d = v_i^c \frac{t_i^c}{t_i^a}$ 
5   if  $v_i^d \geq v^{min}$  then
6      $v_i \leftarrow v_i^d$ 
7      $t_i^w \leftarrow 0$ 
8     Keep original route at speed  $v_i$ 
9   else
10     $v_i \leftarrow v_i^{min}$ 
11     $t_i^w \leftarrow t_i^a - t_i^c \frac{v_i^c}{v_i^{min}}$ 
12     $n_i = \frac{t_i^w \cdot v_i}{L^{seg}}$ 
13    Reroute to delay absorbing circle for  $n_i$  segments.
```

When the required time of arrival (RTA) is updated, the automation system will check the status of aircraft that are in the decision buffer zone or have not yet entered terminal airspace. For each of these aircraft, the desired speed v^d is calculated based on the proportion of cruised flying time t^c and the actual flying time t^a , which is from the time gap between ETA and RTA. If the desired speed is higher than the minimum speed required by the airspace route, the aircraft will receive a command to adjust to the desired speed and process on course. If the desired speed is lower than the minimum speed, the aircraft will maintain the minimum speed and a waiting time t^w will be recorded, representing the time difference between the desired flying time and the actual flying time at the minimum speed without entering the holding pattern. It's worth noting that for aircraft such as eVTOLs, the minimum speed could be zero due to their ability to hover at a location. However, in this case, we have defined the minimum speed as the minimum speed requirement of the airspace route (e.g., 10 knots) to ensure that the aircraft does not hover and consume more battery power. Finally, the number of flying segments with a fixed length L^{seg} will be calculated and assigned to the aircraft. After flying through the required number of segments along the holding pattern, the aircraft will continue its original route until it reaches the nearest holding exit point, at which point it will return to the approach route.

4. Numerical Experiments

4.1 Algorithm Performance Analysis

In our experiment to evaluate the performance of scheduling and separation algorithms, we created traffic demand consisting of 12 aircraft distributed across four arrival routes. Initially, the traffic density is low, then nine aircraft appear almost simultaneously between 900-1,000 seconds.

As shown in Figure 4, the speed curves of the 12 aircraft demonstrate the effectiveness of the separation operations. Without these operations, the top plot shows that 9 aircraft would land with very little separation, which could lead to near mid-air collisions (NMACs) and is not acceptable for vertiport operators. However, after

implementing the separation operations, the bottom plot shows that the arrival times of all the aircraft are spaced out appropriately using different flying speeds and holding times, preventing any potential landing collisions. Table 1 shows the details of the computational results of scheduling and separation algorithms. Here, the in-air delay is the time interval between the original ETA and the actual landing time, while the landing interval is the time interval of adjacent landing time. We observed that the automated system can keep the landing intervals greater than 100 seconds. In addition, with the accumulation of in-air delay, changing speed is not enough to absorb in-air delay, then an extra holding time is introduced for a proper landing separation.

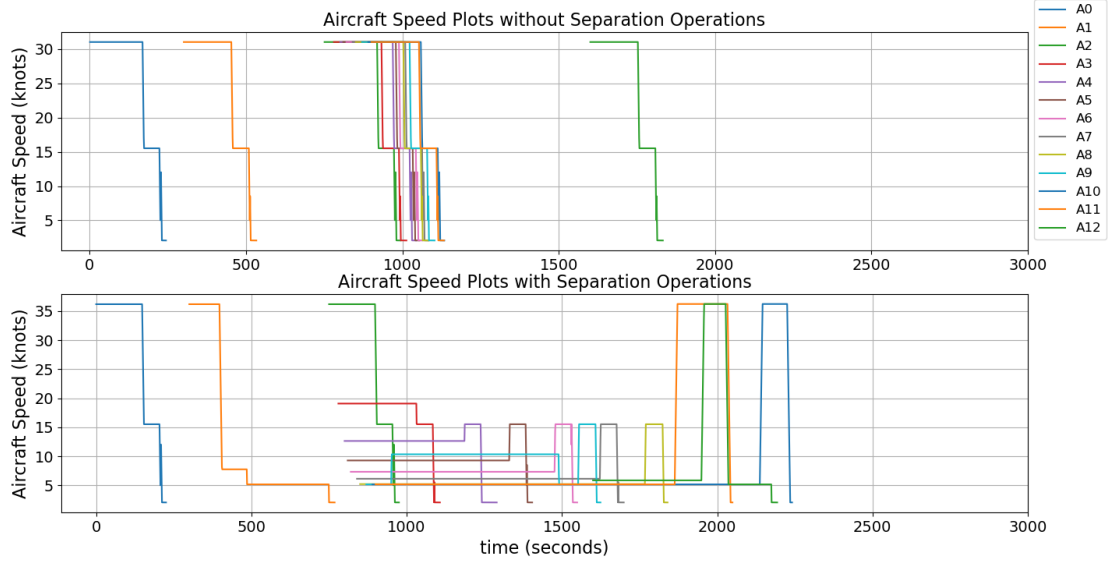


Figure 4: Aircraft speed plot during arrival phase

Table 1: Scheduled and actual operational results

Flight ID	ETA (sec.)	RTA (sec.)	Landing Time (sec.)	In-air Delay (sec.)	Landing Interval (sec.)	Desired Speed (knot)	Holding Time (sec.)
1	244	220	226	0	-	70.0	0
2	544	520	537	0	311	70.0	0
3	994	970	976	0	439	70.0	0
4	1024	1130	1108	84	132	36.8	0
5	1044	1290	1291	247	183	24.4	0
6	1054	1450	1405	351	114	17.9	0
7	1064	1610	1550	486	145	14.2	0
8	1084	1770	1700	616	150	11.9	0
9	1094	1930	1843	749	143	10.1	0
10	1114	2090	2170	1056	327	10.0	131.0
11	1134	2250	2375	1241	205	10.0	271.0
12	1144	2410	2524	1380	149	10.0	421.0

4.2 Sensitivity Analysis

In this experiment, we evaluated the algorithm performance on different traffic

demands. We generated flight appearance intervals randomly by beta distribution on each route. The use of the beta distribution allows us to specify different traffic demands using its shape parameters. The time-varying mean appearance rate of the aircraft is determined using:

$$\lambda(t) = \int_t^{t+1} \lambda'(\tau) A d\tau$$

where $\lambda(t)$ is the appearance rate at time t , A is the total number of flights on each route, and $\lambda'(\tau)$ is the probability density function value of a beta distribution. The probability density function of the beta distribution is defined as:

$$\lambda(\tau) = \frac{\left(\frac{\tau}{T}\right)^{\alpha-1} \left(1 - \frac{\tau}{T}\right)^{\beta-1}}{B(\alpha, \beta)}$$

where

$$B(\alpha, \beta) = \frac{\Gamma(\alpha)\Gamma(\beta)}{\Gamma(\alpha + \beta)}$$

Here, α, β are two parameters to determine appearance curves, and T is the total appearance time. The total appearance time then can be defined as the number of total flights divided by the demand of operations per hour. Thus, by determining the number of flights and giving landing demands, we can generate an appearance timetable of aircraft based on beta distribution.

To demonstrate how the scheduling and separation algorithms function with varying levels of traffic, we evaluated the actual landing interval beyond the current required throughput. For instance, if the current throughput rate is 1 operation per minute, the landing interval should exceed 60 seconds. If the actual landing interval between two aircraft is 20 seconds, then the *landing intervals over throughput (LIOT)* would be 40 seconds. If the landing interval is above the required interval, it will be counted as zero.

In this experiment, we choose $\alpha = 2, \beta = 4$, and generate 8 aircraft on each route, for a total of 32 operations. We evaluated appearance demands from low to high, as shown in Figure 5.

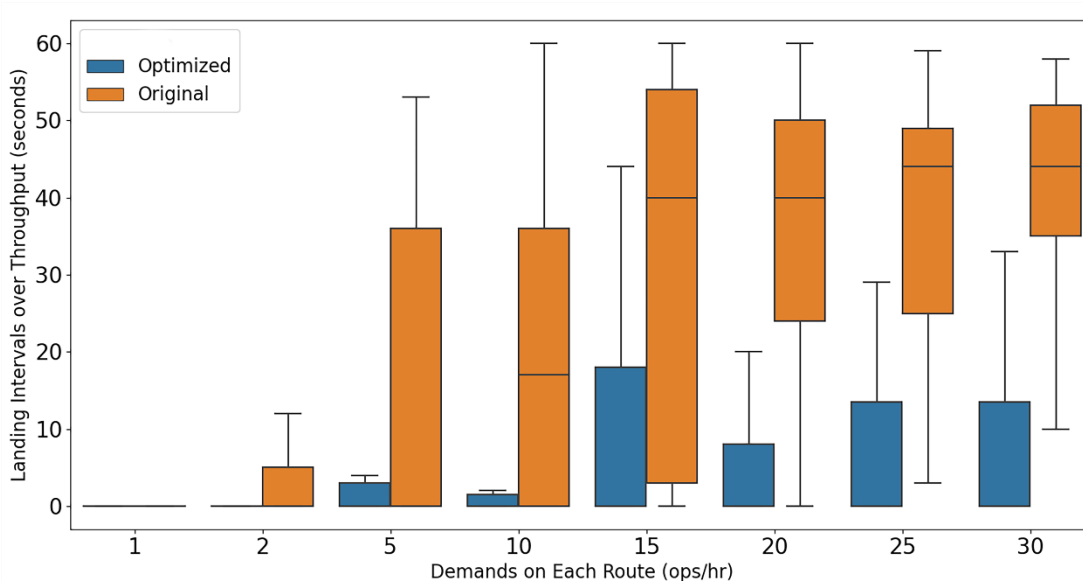


Figure 5: Landing intervals on varying arrival demands

Figure 5 demonstrates that the scheduling and separation algorithms, when compared to the original traffic flow, can effectively reduce landing conflicts, resulting in a consistently zero median of LIOT. However, it is worth noting that this method cannot eliminate all conflicts. This is primarily due to high traffic density, which causes most aircraft to enter holding patterns. Based on the current setting, the holding pattern is divided into several discrete segments, and aircraft cannot leave the holding pattern until they reach the nearest holding exit point, which creates a time gap between the required time of arrival and the actual landing time. This uncertainty is the primary cause of LIOT for automated system.

5. Conclusion

As the FAA defines operational constraints for managing the traffic and conflicts in and around the vertiport, V-HATT demonstrates degree of automation required to manage large volumes of AAM aircraft to meet those constraints under various operating conditions. This paper describes the automated system in V-HATT, which integrates the optimization-based scheduling algorithm and maneuvers advisory algorithms to mitigate landing conflicts around the high-density terminal airspace. The results suggest that the holding pattern could satisfy operational efficiency because it could absorb in-air delay in high-density space-limited airspace. The paper also suggests that the scheduling and separation algorithms could be an efficient tool for vertiport operators to resolve conflicts and increase the vertiport throughput.

6. Future Work

The next step will integrate departure schedules into the system. Further research could involve testing the robustness of the system by introducing additional sources of uncertainty - such as delayed flights, variable flight performance, and dynamic weather conditions.

Acknowledgement

This work was completed under a National Aeronautics and Space Administration Small Business Innovative Research Phase I contract number 80NSSC22PB003, “Vertiport Human Automation Teaming Toolbox (V-HATT) Phase I Final Report.” The authors thank the NASA contract monitor, Ms. Savita Verma, for her guidance during this project.

References

- Crown Consulting. 2023. "Vertiport Human Automation Teaming Toolbox (V-HATT) Phase I Final Report." Alexandria, VA.
- Hoekstra, Jacco M., and Joost Ellerbroek. 2016. "Bluesky ATC simulator project: an open data and open source approach." *In Proceedings of the 7th international conference on research in air transportation*. USA/Europe: FAA/Eurocontrol. vol. 131, p. 132.
- Lee, Hanbong, Kushal A. Moolchandani, and Heather Arneson. 2022. "Demand capacity balancing at vertiports for initial strategic conflict management of urban air mobility operations." *2022 IEEE/AIAA 41st Digital Avionics Systems Conference (DASC)*. IEEE. pp. 1-10.
- Mendonca, Nancy, James Murphy, Michael D. Patterson, Rex Alexander, Gabriela Juarex, and Clint Harper. 2022. "Advanced Air Mobility Vertiport Considerations: A List and Overview." *AIAA AVIATION 2022 Forum*. p. 4073.
- Northeast UAS Airspace Integration Research Alliance, Inc. 2021. "High-Density Automated Vertiport Concept of Operations." Rome, NY.
- Pradeep, Priyank, and Peng Wei. 2018. "Heuristic approach for arrival sequencing and scheduling for eVTOL aircraft in on-demand urban air mobility." *2018 IEEE/AIAA 37th Digital Avionics Systems Conference (DASC)*. IEEE. pp. 1-7.
- The Federal Aviation Administration. 2022. "Charting Aviation's Future: Operations in an Info-Centric National Airspace System." Washington, DC.
- The Federal Aviation Administration. 2022. "Engineering Brief No. 105, Vertiport Design." Washington, DC.